• Basic Research •

Effects of chronic elevated intraocular pressure on parameters of optical coherence tomography in rhesus monkeys

Zhi-Chao Yan[1,2], Xue-Jiao Yang[3], Hong-Rui Chen[2], Shui-Feng Deng[2], Ying-Ting Zhu[2], Ye-Hong Zhuo[2]

[1]Department of Ophthalmology, the Second Affiliated Hospital of Guangzhou Medical University, Guangzhou 510260, Guangdong Province, China

[2]State Key Laboratory of Ophthalmology, Zhongshan Ophthalmic Center, Sun Yat-sen University, Guangzhou 510060, Guangdong Province, China

[3]Department of Ophthalmology, the Affiliated Hospital of Qingdao University, Qingdao 266000, Shandong Province, China

Co-first authors: Zhi-Chao Yan and Xue-Jiao Yang

Correspondence to: Ye-Hong Zhuo. State Key Laboratory of Ophthalmology, Zhongshan Ophthalmic Center, Sun Yat-sen University, 54 South Xianlie Road, Guangzhou 510060, Guangdong Province, China. zhuoyh@mail.sysu.edu.cn

Received: 2018-06-10 Accepted: 2018-10-09

Abstract

• AIM: To determine the progression of parameters from optical coherence tomography (OCT) in chronic elevated intraocular pressure (IOP) monkeys.

• METHODS: A chronic elevated IOP model of rhesus monkeys was induced by laser photocoagulation. Representative OCT parameters, including the average and four-quadrant retinal nerve fiber layer (RNFL) thickness, and parameters from optic nerve head (ONH) analysis were collected before and after laser treatments biweekly for up to 28wk. The performance of each parameter for early progression detection was analyzed. The progressive trends toward elevated IOP were analyzed using a linear mixed-effects model.

• RESULTS: There were 10 successfully maintained high IOP eyes in 7 monkeys. The follow-up time was 24±5.37wk. With cumulative IOP elevation, the cup area, rim area and C/D area ratio were statistically significantly changed as early as 2wk after elevated IOP induction (P<0.05). The quadrant RNFL thickness changed at 6wk after high IOP induction, and the superior and inferior RNFL thicknesses exhibited more obvious reductions than other quadrants. The average RNFL thickness was the last one to show a significant decrease at 8wk.

• CONCLUSION: The parameters of ONH are most sensitive to elevated IOP in a primate glaucomatous model. These findings suggest that we should focus on those parameters instead of RNFL thickness in patients with elevated IOP, as they might present with earlier glaucomatous changes.

• KEYWORDS: optical coherence tomography; rhesus monkey; glaucoma; high intraocular pressure; retinal nerve fiber layer

DOI:10.18240/ijo.2019.04.03

Citation: Yan ZC, Yang XJ, Chen HR, Deng SF, Zhu YT, Zhuo YH. Effects of chronic elevated intraocular pressure on parameters of optical coherence tomography in rhesus monkeys. *Int J Ophthalmol* 2019;12(4):542-548

INTRODUCTION

Glaucoma is a leading cause of irreversible blindness worldwide[1]. The condition is called "the silent thief of sight" due to its chronic progression without any notice, particularly primary open angle glaucoma (POAG). Studies have shown that early detection and early intervention are the best ways to prevent vision loss[2]. Therefore, it is of great importance to recognize early glaucoma progression.

Elevated intraocular pressure (IOP) is the most important risk factor for glaucoma progression[3]. However, it is unethical and difficult to study the effects of elevated IOP on damaged fundus in human beings instead of treatment. Compared with rodents, monkeys and humans have close phylogeny and high homology[4]; therefore, the rhesus monkey was used in our study. Previous studies have shown that laser photocoagulation of the trabecular meshwork can be used to induce IOP elevation in monkeys, which is an ideal model to study the effect of elevated IOP and to investigate glaucoma progression[5-6].

Structural and functional damages are seen in early glaucoma or glaucoma progression detection during clinical practice, in which optic coherence tomography (OCT) and visual field (VF) are most widely used[7-9]. Studies have shown that structural changes can be detected earlier than functional

change[8-9]. With the maturation of big data collection methods, it is easy to get large amounts of data from various devices; however, analyzing and applying them in clinical practice is challenging.

Many studies have been conducted to characterize the structural progression under cumulative high IOP, and various apparatus with various parameters have been used, such as OCT, confocal laser scanning ophthalmoscope (CLSO), scanning laser perimetry (SLP), *etc*[10-13]. However, regarding RNFL thickness analysis, the "average RNFL thickness" has been commonly used, which is an overall parameter without considering the separate changes occurring in each quadrant of the peripapillary RNFL thickness[5,10,12-13]. Moreover, some studies have made comparisons of some parameters from different apparatus[11]. In clinical practice, it might be more helpful for us to achieving a thorough understanding of the earlier progression trend of each parameter, and to understanding the effect of elevated IOP on the early progression of parameters from fundus scanning, and to conducting the earlier intervention.

Our research group has successfully established stable chronic high IOP monkey models with similar laser photocoagulation of the trabecular meshwork[14]. In this study, we conducted a full analysis of the progression of different parameters of OCT in a longitudinal study with trend analysis and relative long-term follow-up. The aim of this study was to determine the performance of progression detection of each parameter, which may offer guidance in applying various OCT parameters for glaucomatous monitoring in clinical practice.

MATERIALS AND METHODS

Ethical Approval This study strictly adhered to the ARVO Statement for the Use of Animals in Ophthalmic and Vision Research. It was approved and monitored by the Institutional Animal Care and Use Committee of Zhongshan Ophthalmic Center.

Materials Seven healthy adult rhesus monkeys (Blue Island Biological Technology Co., Ltd., of Guangdong, Guangzhou, China, Qualification), with initial body weights of 7-12 kg and initial ages of 5-6y, were used in this study. Before creating models, monkeys were examined using various tests to confirm the healthy state of their eyes, including slit-lamp microscopy (Topcon, SL-D7, Japan), gonioscopic examination (Volk G-1 trabeculum, Volk Optical, Inc., Mentor, OH, USA), fundus photography (TRC-50DX Retinal Camera; Topcon, Tokyo, Japan), OCT (Stratus OCT, Carl Zeiss Meditec, Dublin, CA, USA), and Tono-Pen XL tonometry (Reichert, Depew, NY, USA).

Establishment of the Model Detailed descriptions of model establishment have been previously published[14]. Briefly, after anesthesia, laser-dedicated gonioscopy (Volk, G-1 Trabeculum, USA), multiwavelength solid-state lasers and associated multiplier slit-lamp microscopes (VISULAS Trion & LSL Trion Laser Slit Lamp, Carl Zeiss Meditec AG, Goeschwitzer Strasse, Jena, Germany) were used to perform 360° photocoagulation in the functional trabecular meshwork area of each eye in all subjects. The laser spot size was 50 μm in diameter, and the settings were 1200 W for 0.5s. Laser parameters were adjusted to obtain a visible reaction in the trabecular meshwork, most often a bubble formation. Eighty to 120 spots were created per treatment. Daily application of tobramycin dexamethasone eye drops (TobraDex, Alcon, USA) was performed once a day after each laser procedure for two weeks. Inclusion criteria: the eyes with IOP consistently between 25-40 mm Hg for more than 8wk were included for further analysis.

Intraocular Pressure Measurement After laser photocoagulation, Tono-PenXL was used for the measurement of IOP. During the first 2wk after laser treatment, the IOP was monitored every week, and then biweekly. The apparatus was corrected before each measurement, the IOP measurements were taken 4 times, and the average data were regarded as the IOP of the day. If the IOP was not consistently higher than 25 mm Hg within a week, additional laser treatment was performed until stable ocular hypertension was achieved. The IOPs of recruited monkeys were between 25-40 mm Hg.

Fundus and Optic Coherence Tomography Examinations Animals were anesthetized with an intramuscular injection of ketamine hydrochloride (10-20 mg/kg, Ketalar 50®, GuTian Pharmaceuticals Ltd., Fujian, China) plus chlorpromazine hydrochloride (3.5 mg/kg, Ketalar 50®, GuTian Pharmaceuticals Ltd, Fujian, China). Pupils were dilated using one drop of tropicamide compound (Mydrin-P, Santen Pharmaceutical Co., Ltd., Japan) before fundus photography and OCT scanning. The bilateral fundus of each animal were photographed using an ocular fundus camera (TRC-50DX Retinal Camera; Topcon, Tokyo, Japan) before and after laser photocoagulation to record the overall findings of the optic nerve head (ONH), such as cupping, rim hemorrhage, and other features. At the same time, eyes were scanned by commercially available Stratus OCT (Carl Zeiss Meditec, Dublin, CA, USA) biweekly. Timolol was used for lowering the IOP before OCT scanning. The fast-scanning mode of peripapillary retinal nerve fiber layer (RNFL) thickness and the optic disc protocol were used for analysis. Artificial tears were applied if necessary to maintain the wetness of the ocular surface. At each imaging record, at least two images were acquired from each subject to achieve the best focus. The image with the higher quality was selected for analysis.

Protocol and Parameters

Fast retinal nerve fiber layer scanning Each image consisted of 3 sets of 256 A-scans along a 3.4-mm diameter

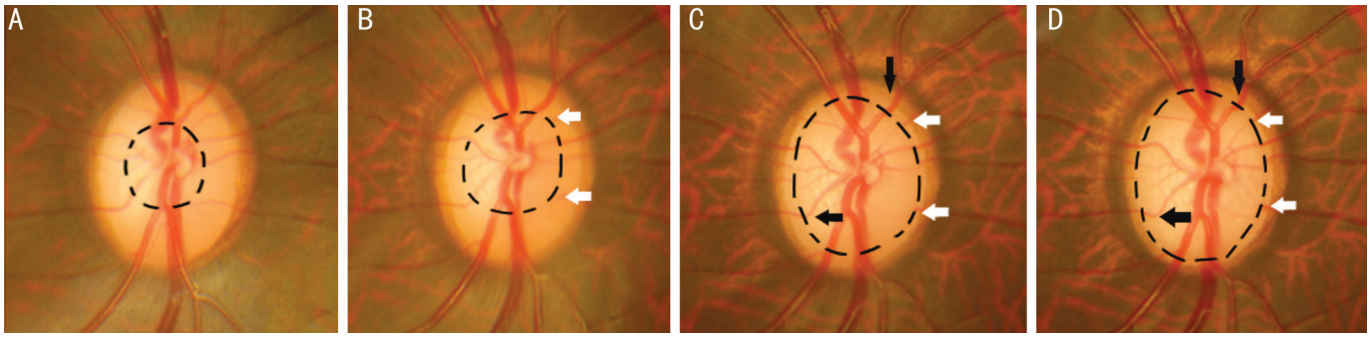

Figure 1 Enlargement of the cup on the ONH in chronic high IOP monkey models A to D present the original fundus photos taken before and 10, 20, and 28wk after laser coagulation, respectively. Photos were overlapped with the lining of the optic cup, which is easily detected under slit lamp combined with lens. A: The ONH before laser coagulation, with a cup to disc ratio (C/D) of 0.3; B: The progression at 10wk after high IOP, C/D=0.6; C, D: The late stages of glaucoma progression at 20 and 28wk after high IOP, respectively, with C/D ratios of approximately 0.8-0.9. Black arrows show the bending of blood vessels on the optic disc. White arrows show the interruption of capillary blood vessels on the optic disc.

circumpapillary scan centered at the ONH. Under its RNFL analysis protocol, the device automatically determines the RNFL anterior and posterior boundaries, peripapillary RNFL thickness parameters, including average thickness (360°), superior, nasal, inferior, and temporal quadrant thickness, were recorded and evaluated in this study. These values were provided in the printout after averaging the results of 3 sequential circular scans captured during acquisition[15].

Fast optic disc scanning A set of 6 radial intersecting line scans, each at 30-degree intervals, were obtained in a single alignment and capture operation such that each clock hour of the optic nerve was scanned. The topography of the entire optic disc was computed by interpolating to fill the gaps between radial linear scans[16]. From all of the parameters of the printout, the three representative optic disc parameters of cup area, rim area and cup to disc (C/D) area ratio were selected for analysis.

Cup area: surface area bounded by the outline of the optic cup; this outline is determined by locating the cup diameter in each linear scan by a line that is located 150 μm anterior to the disc diameter line and connecting the cup diameter marker for each clock hour. Rim area: surface area calculated by subtracting the cup area from the disc area. C/D area ratio: ratio of the cup area to the disc area.

All of the above-mentioned parameters from both protocols were recorded to analyze their changes with increased IOP and follow-up duration.

Statistical Methods R software package 3.3.2 (R Foundation for Statistical Computing, Vienna) was used for all of the analyses. The linear mixed-effects model was used for analyzing the time point at which statistically significant changes developed for all of the parameters, including the average and four-quadrant RNFL thickness, cup area, rim area, and C/D area ratio, with the elevated IOP and follow-up duration. Two nested random factors were introducing into our model since repeated measures were made on the same eye, and two eyes were sometimes measured from the same subject.

Table 1 The demographic characteristics of the involved rhesus monkeys

Animal No.	Sex	Age (y)	Baseline IOP (mm Hg)		Fellow-up time (wk)
			Right eye	Left eye	
1	Male	6	15.6667	-	14
2	Male	6	17	-	28
3	Male	6	-	15	28
4	Male	6	-	10.333	14
5	Male	5	20	18.5	28
6	Female	5	21	18	24
7	Male	5	22	19	28

RESULTS

Chronic elevated IOP animal models were successfully established by laser photocoagulation of the trabecular meshwork on ten eyes of 7 monkeys (both pairs of eyes from 3 monkeys and single eyes from the other monkeys). The demographic characteristics of the involved rhesus monkeys are shown in Table 1. The appearance of ONH and the peripapillary RNFL thickness change at corresponding time points are shown in Figures 1 and 2, respectively. As time progressed, the optic cup was enlarged, and the color of the ONH was pale, with distinctive bending or disrupture of capillary blood vessels. The RNFL thickness became thinner and thinner, with the characteristic “double hump” curve lowered as time progressed.

Parameters Before Laser Treatment Relevant parameters before laser treatment, including IOP and all of the selected parameters of OCT, are presented in Table 2. The normal IOP of rhesus monkeys is almost the same as that of human beings, with the average IOP being 17.6 mm Hg and ranging from 10.3 to 22 mm Hg.

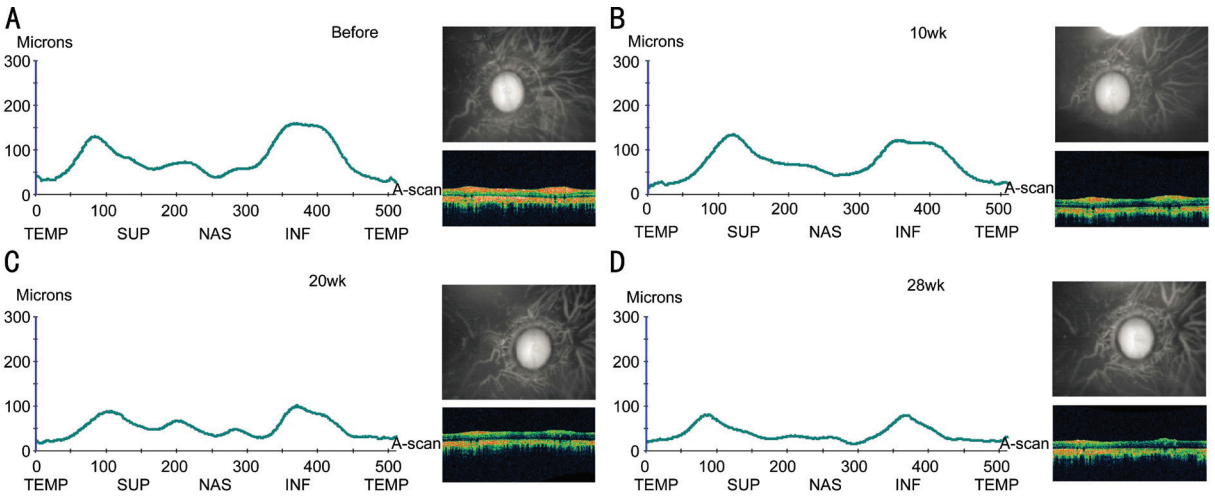

Figure 2 RNFL thickness changes in a chronic high IOP monkey model of disease progression with increased IOP and time duration A to D show the OCT reports taken before and 10, 20, and 28wk after laser coagulation, respectively. With increasing time from A to D, the RNFL thickness decreased, and the characteristic "double hump" curve became lower and lower.

Table 2 Descriptive data of IOP and OCT parameters from rhesus monkeys before laser coagulation

Parameter	*n*	Min	Max	Mean	SD
IOP (mm Hg)	10	10.3	22	17.6	3.39
RNFL-Avg (μm)	10	79	103	89.7	8.91
RNFL-S (μm)	10	88	131	107.8	13.66
RNFL-I (μm)	10	110	159	132.2	14.47
RNFL-N (μm)	10	44	97	60	15.55
RNFL-T (μm)	10	44	78	64.3	12.66
Cup area (mm^2)	10	0.3	1.7	0.8	0.42
Rim area (mm^2)	10	0.9	2.3	1.5	0.46
C/D area ratio	10	0.1	0.6	0.4	0.16

RNFL: Retinal nerve fiber layer; RNFL-Avg: Average RNFL thickness; RNFL-S: Superior quadrant RNFL thickness; RNFL-I: Inferior quadrant RNFL thickness; RNFL-N: Nasal quadrant RNFL thickness; RNFL-T: Temporal quadrant RNFL thickness; C/D area ratio: Cup to disc area ratio.

Changes of Parameters Under Intraocular Pressure Elevation The changes of OCT parameters in the 10th and 28th weeks after IOP elevation compared with their baseline data are shown in Table 3. The superior RNFL thickness was reduced by 25.333 μm at 10wk and 43.6 μm at 28wk compared with the baseline. The inferior RNFL thickness was reduced by 34.333 μm at 10wk and 64 μm at 28wk compared with the baseline.

Progression Trends of Various Parameters over Time After Establishment of the Model The follow-up time of recruited rhesus monkeys was 24±5.37wk after IOP elevation. As is shown in Figure 3, there was moderate elevation of IOP levels in monkeys of approximately 30-40 mm Hg.

The progression trends of RNFL thickness, including average, superior, inferior, nasal and temporal quadrant RNFL thickness, are shown in Figure 4. All of the thickness

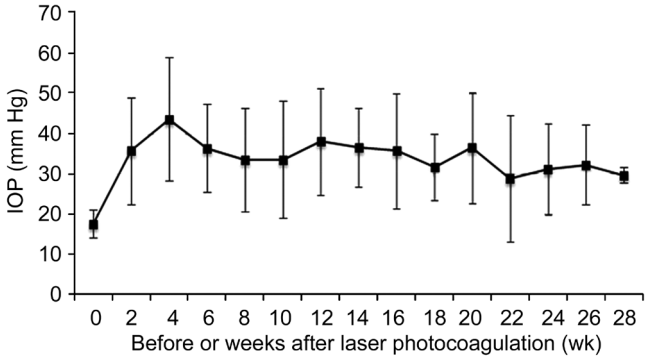

Figure 3 Means and standard deviations of IOP before and after establishment of the high IOP model in rhesus monkeys On the horizontal axis, 0 represents the IOP before laser photocoagulation, and the other axis marks represent weeks after laser photocoagulation.

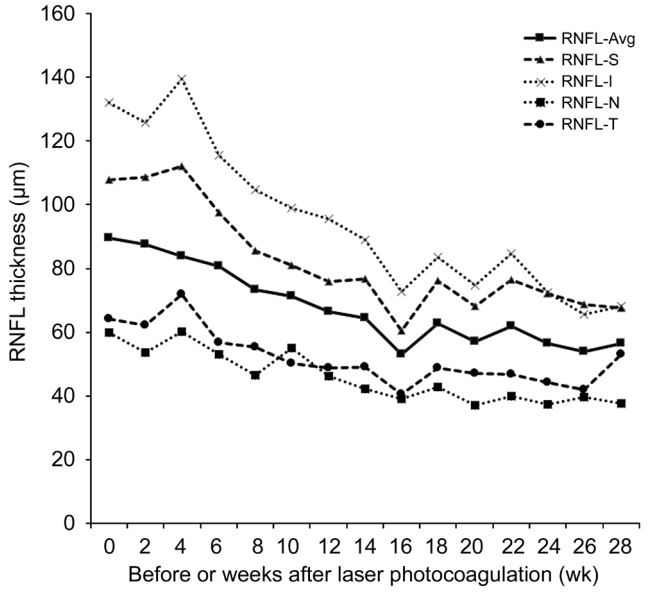

Figure 4 RNFL thicknesses before and after establishment of the high IOP model in rhesus monkeys On the horizontal axis, 0 represents the IOP before laser photocoagulation, and the other axis marks represent weeks after laser photocoagulation.

Table 3 Changes in OCT parameters in the 10th and 28th week after IOP elevation compared with the baseline data mean±SD

Parameter	No. of eyes	0 wk	10-0 wk[a]	28-0 wk[b]
RNFL-Avg (μm)	10	89.7±8.908	-18.222±24.144	-34.8±28.341
RNFL-S (μm)	10	107.8±13.661	-25.333±40.841	-43.6±34.717
RNFL-I (μm)	10	132.2±14.474	-34.333±38.331	-64±41.407
RNFL-N (μm)	10	60±15.549	-6.444±19.236	-27.2±26.781
RNFL-T (μm)	10	64.3±12.658	-12.889±20.817	-14±33.174
Cup area (mm^2)	10	0.83±0.425	0.91±0.82	1.112±0.625
Rim area (mm^2)	10	1.513±0.456	-0.629±0.62	-0.682±0.526
C/D area ratio	10	0.354±0.165	0.278±0.248	0.307±0.196

RNFL: Retinal nerve fiber layer; RNFL-Avg: Average RNFL thickness; RNFL-S: Superior quadrant RNFL thickness; RNFL-I: Inferior quadrant RNFL thickness; RNFL-N: Nasal quadrant RNFL thickness; RNFL-T: Temporal quadrant RNFL thickness; C/D area ratio: Cup to disc area ratio. [a]Changes of each parameters at 10th week compared with baseline; [b]Changes of each parameters at 28th week compared with baseline.

Table 4 Progression rates of parameters from OCT over time in the high IOP rhesus monkey model

Parameter	Earliest change[c]	Primary progression rate (/2wk)[a]	95%CI	*P*	Overall progression rate (/2wk)[b]	95%CI	*P*
RNFL-Avg (μm)	8wk	-16.15	-28.822, -3.477	0.015	-31.464	-49.635, -13.293	0.006
Cup area (mm^2)	2wk	0.428	0.081, 0.776	0.018	1.135	0.63, 1.64	<0.001
Rim area (mm^2)	2wk	-0.277	-0.548, -0.005	0.049	-0.728	-1.274, -0.181	0.091
C/D area ratio	2wk	0.463	0.086, 0.841	0.018	1.262	0.627, 1.896	0.011

RNFL-Avg: Average retinal nerve fiber layer thickness; C/D area ratio: Cup to disc area ratio. [a]The primary progression rate till there is a statistically significant change; [b]The entire progression rate until the last follow-up. [c]The earliest time point that show statistically significant change.

parameters decreased with time. In the early stages, the RNFL thicknesses of the superior and inferior quadrants were larger than those of the other two quadrants, and they were severely damaged compared with the others. After 16wk, the progression trends of all parameters became slow, possibly due to the "floor effect" of RNFL thickness damage.

Analysis of Relevant Parameters As is shown in Table 4, in the statistical trend analysis, we found the following results. First, the ONH analysis parameters, including cup area, rim area and C/D area ratio, were the first three parameters that presented statistically significant changes, which occurred 2wk after IOP elevation in monkeys. Second, quadrant RNFL thickness parameters, including superior, inferior, nasal and temporal quadrant RNFL thicknesses, were the next parameters to show statistically significant changes at 6wk after IOP elevation (Table 5). Compared with the superior RNFL thickness, the inferior and nasal RNFL thicknesses were significantly different, but with less influence. Finally, the average RNFL thickness was significantly changed at 8wk.

Table 5 Comparison of the progression rates of different quadrant RNFL thicknesses over time in the high IOP rhesus monkey model

Duration	Slope	95%CI	*P*
2wk	4.99	-5.221, 15.202	0.339
4wk	-5.2	-15.541, 5.141	0.325
6wk[a]	-12.281	-23.107, -1.456	0.027[a]
8wk	-14.075	-24.898, -3.252	0.011
10wk	-22.59	-33.399, -11.78	<0.001
12wk	-23.257	-34.034, -12.48	<0.001
14wk	-27.643	-39.445, -15.84	<0.001
16wk	-22.303	-34.108, -10.499	<0.001
18wk	-27.821	-39.058, -16.583	<0.001
20wk	-23.248	-34.114, -12.382	<0.001
22wk	-28.534	-39.761, -17.307	<0.001
24wk	-31.237	-43.05, -19.424	<0.001
26wk	-28.566	-43.776, -13.357	<0.001
28wk	-9.952	-16.179, -3.724	0.002
RNFL-I[b]	10.654	4.426, 16.881	0.001
RNFL-N[b]	13.192	6.965, 19.42	<0.001
RNFL-T[b]	4.99	-5.221, 15.202	0.339

RNFL: Retinal nerve fiber layer; RNFL-I: Inferior quadrant RNFL thickness; RNFL-N: Nasal quadrant RNFL thickness; RNFL-T: Temporal quadrant RNFL thickness. [a]The RNFL thickness began to have significant change at 6wk after high IOP; [b]This parameter was compared with the superior RNFL thickness.

DISCUSSION

This study was designed to investigate the dynamic progression of structural parameters from OCT under IOP elevation. Representative parameters were analyzed in rhesus monkeys with chronic elevated IOP with 28wk of follow-up. We found that with cumulative IOP elevation and follow-up duration, parameters from ONH analysis, including cup area, rim area and C/D area ratio, were the first three parameters to show statistically significant differences as early as 2wk after IOP elevation. RNFL thicknesses, including both average and quadrant RNFL thicknesses, were damaged later under high

IOP. These facts suggest that more attention should be paid to these three parameters instead of RNFL thickness during clinical practice, especially for ocular hypertension patients, as these changes might occur at early stages of glaucomatous fundus damage.

In the normal human eye, RNFL thickness showed a double-hump pattern, with relatively similar superior and inferior peaks and with temporal and nasal troughs[17]. This structure was confirmed in both *in vivo* imaging[18] and normal histologic eyes[17], while in glaucomatous eyes, the bulk of glaucomatous damage to the RNFL thickness occurs in the superior and inferior quadrants[19-21]. Our study shows a similar tendency in glaucomatous monkeys, as the superior and inferior RNFL thicknesses were initially reduced compared with other quadrants. Previous studies suggested that superior and inferior parts of the lamina at the level of the sclera appeared to contain larger pores and thinner connective tissue support for the passage of nerve-fiber bundles (*i.e.* dense arcuate retinal ganglion cell axons) than the nasal and temporal parts of the lamina[22-23]. These areas are more susceptible to glaucomatous damage, such as IOP elevation, which might explain the characteristic pattern of early glaucomatous field loss.

Early diagnosis or detection of glaucomatous progression is critical for taking effective measures for visual function protection. However, it is difficult to observe the process of progression from the eye's normal state to glaucomatous damage (the earliest change) in patients. Structural and functional examinations are two effective procedures for monitoring and evaluation of glaucoma[7-9]. OCT has been shown to obtain accurate and reproducible RNFL and retinal thickness measurements that correspond to histomorphometric measurements of the same tissues[24-25]. Wollstein *et al*[26] found that OCT is more sensitive for showing glaucomatous damage compared with VF. Another longitudinal study[9] demonstrated that the average and inferior quadrant RNFL thicknesses showed statistically significant changes compared with other parameters during glaucoma progression, which partially corresponded with our results.

There are many parameters on OCT reports, but it is difficult to differentiate normal from abnormal results since there is no widely used database for rhesus monkeys. In our study, the glaucomatous damage was detected by trend analysis, in which the baseline state was compared with the progression process itself. Moreover, this method removes the effects of individual differences. With trend analysis, we obtained progression rates up to half a year (28wk), and all selected parameters showed statistically significant progression (P<0.05). The knowledge of these progression rates contributes to understanding the process of glaucomatous fundus damage under IOP elevation, which is impossible for us to study in human beings.

Regarding the changes of ONH under IOP elevation, several researchers have analyzed relevant parameters by HRT or SD-OCT and discovered that the rim area was significant in patients with glaucoma progression[27-28]. In our study, the representative parameters of ONH, including cup area, rim area and C/D area ratio, were decreased at 2wk after IOP elevation. It is reasonable that the damage occurred first on ONH and then progressed to the RNFL. Therefore, we suggest that in clinical practice, parameters from ONH should be prioritized over other parameters scanned by OCT[27-28].

There are some inconsistencies between the results of our study on monkeys and other studies on patients. In addition to the species difference, the reason for these inconsistencies might be that glaucomatous progression in patients may be far more complex than a single high IOP effect, including ischemia of the optic nerve, low infusion, primary or secondary inflammation or immune mechanisms, intraocular growth factors, ROS, and other contributing factors, which might have some influence on RNFL thickness or ONH. At the late stage of glaucomatous optic neuropathy, inflammation or immune-related signaling pathways, including autophagy activity[29] and apoptosis, might lead to secondary optic nerve damage to accompany the primary damage. Therefore, our study revealed the pure effects of high IOP on glaucomatous structural changes at very early stages, which might help us identify the real damage of single elevated IOP to the fundus. Additionally, our study shows the process from a normal state to a glaucomatous damaged state, other than the progression from an early stage to a late stage of disease, as later stages might involve some of the other above-mentioned complex mechanisms.

In summary, our study used trend-based analysis to investigate longitudinally the effects of chronic elevated IOP on OCT parameters with a rhesus monkey model induced by laser photocoagulation of the trabecular meshwork, which lay an experimental basis for the further study of the contributions of glaucomatous structural, functional and molecular biological damage in glaucoma. In addition, the detection of the progression of each parameter under cumulative IOP elevation provides guidance for glaucomatous monitoring during clinical practice.

ACKNOWLEDGEMENTS

The authors would like to thank Dr. Zhi-Cheng Du for assistance with statistics.

Foundations: Supported by National Natural Science Foundation of China (No.81470627; No.81600726); Shandong Province Natural Science Foundation (No.ZR2016HB53); Natural Science Foundation of Guangdong Province (No.2018A030310185); the Research Funding of Guangzhou Medical University (No.2016C21).

Conflicts of Interest: Yan ZC, None; **Yang XJ,** None; **Chen HR,** None; **Deng SF,** None; **Zhu YT,** None; **Zhuo YH,** None.

REFERENCES

1 Lee DA, Higginbotham EJ. Glaucoma and its treatment: a review. *Am J Health Syst Pharm* 2005;62(7):691-699.

2 The Advanced Glaucoma Intervention Study (AGIS): 7. The relationship between control of intraocular pressure and visual field deterioration. The AGIS Investigators. *Am J Ophthalmol* 2000;130(4):429-440.

3 Wax MB, Camras CB, Fiscella RG, Girkin C, Singh K, Weinreb RN. Emerging perspectives in glaucoma: optimizing 24-hour control of intraocular pressure. *Am J Ophthalmol* 2002;133(6):S1-S10.

4 Bouhenni RA, Dunmire J, Sewell A, Edward DP. Animal models of glaucoma. *J Biomed Biotechnol* 2012;2012:692609.

5 Schuman JS, Pedut-Kloizman T, Pakter H, Wang N, Guedes V, Huang L, Pieroth L, Scott W, Hee MR, Fujimoto JG, Ishikawa H, Bilonick RA, Kagemann L, Wollstein G. Optical coherence tomography and histologic measurements of nerve fiber layer thickness in normal and glaucomatous monkey eyes. *Invest Ophthalmol Vis Sci* 2007;48(8):3645-3654.

6 Hayreh SS, Pe'er J, Zimmerman MB. Morphologic changes in chronic high-pressure experimental glaucoma in rhesus monkeys. *J Glaucoma* 1999;8(1):56-71.

7 Wessel JM, Horn FK, Tornow RP, Schmid M, Mardin CY, Kruse FE, Juenemann AG, Laemmer R. Longitudinal analysis of progression in glaucoma using spectral-domain optical coherence tomography. *Invest Ophthalmol Vis Sci* 2013;54(5):3613-3620.

8 Wollstein G, Kagemann L, Bilonick RA, Ishikawa H, Folio LS, Gabriele ML, Ungar AK, Duker JS, Fujimoto JG, Schuman JS. Retinal nerve fibre layer and visual function loss in glaucoma: the tipping point. *Br J Ophthalmol* 2012;96(1):47-52.

9 Sehi M, Zhang X, Greenfield DS, Chung Y, Wollstein G, Francis BA, Schuman JS, Varma R, Huang D, Advanced Imaging for Glaucoma Study G. Retinal nerve fiber layer atrophy is associated with visual field loss over time in glaucoma suspect and glaucomatous eyes. *Am J Ophthalmol* 2013;155(1):73-82.e1.

10 Fortune B, Burgoyne CF, Cull G, Reynaud J, Wang L. Onset and progression of peripapillary retinal nerve fiber layer (RNFL) retardance changes occur earlier than RNFL thickness changes in experimental glaucoma. *Invest Ophthalmol Vis Sci* 2013;54(8):5653-5661.

11 He L, Yang H, Gardiner SK, Williams G, Hardin C, Strouthidis NG, Fortune B, Burgoyne CF. Longitudinal detection of optic nerve head changes by spectral domain optical coherence tomography in early experimental glaucoma. *Invest Ophthalmol Vis Sci* 2014;55(1):574-586.

12 Patel NB, Sullivan-Mee M, Harwerth RS. The relationship between retinal nerve fiber layer thickness and optic nerve head neuroretinal rim tissue in glaucoma. *Invest Ophthalmol Vis Sci* 2014;55(10):6802-6816.

13 Wang L, Burgoyne CF, Cull G, Thompson S, Fortune B. Static blood flow autoregulation in the optic nerve head in normal and experimental glaucoma. *Invest Ophthalmol Vis Sci* 2014;55(2):873-880.

14 Yan Z, Tian Z, Chen H, Deng S, Lin J, Liao H, Yang X, Ge J, Zhuo Y. Analysis of a method for establishing a model with more stable chronic glaucoma in rhesus monkeys. *Exp Eye Res* 2015;131:56-62.

15 Sehi M, Bhardwaj N, Chung YS, Greenfield DS, Advanced Imaging for Glaucoma Study Group. Evaluation of baseline structural factors for predicting glaucomatous visual-field progression using optical coherence tomography, scanning laser polarimetry and confocal scanning laser ophthalmoscopy. *Eye (Lond)* 2012;26(12):1527-1535.

16 Marsh BC, Cantor LB, WuDunn D, Hoop J, Lipyanik J, Patella VM, Budenz DL, Greenfield DS, Savell J, Schuman JS, Varma R. Optic nerve head (ONH) topographic analysis by stratus OCT in normal subjects: correlation to disc size, age, and ethnicity. *J Glaucoma* 2010;19(5):310-318.

17 Cohen MJ, Kaliner E, Frenkel S, Kogan M, Miron H, Blumenthal EZ. Morphometric analysis of human peripapillary retinal nerve fiber layer thickness. *Invest Ophthalmol Vis Sci* 2008;49(3):941-944.

18 Essock EA, Sinai MJ, Fechtner RD, Srinivasan N, Bryant FD. Fourier analysis of nerve fiber layer measurements from scanning laser polarimetry in glaucoma: emphasizing shape characteristics of the 'double-hump' pattern. *J Glaucoma* 2000;9(6):444-452.

19 Shin JW, Uhm KB, Seong M, Lee DE. Retinal nerve fiber layer volume measurements in healthy subjects using spectral domain optical coherence tomography. *J Glaucoma* 2014;23(8):567-573.

20 Wang X, Li S, Fu J, Wu G, Mu D. Comparative study of retinal nerve fibre layer measurement by RTVue OCT and GDx VCC. *Br J Ophthalmol* 2011;95(4):509-513.

21 Maurice C, Friedman Y, Cohen MJ, Kaliner E, Mimouni M, Kogan M, Blumenthal EZ. Histologic RNFL thickness in glaucomatous versus normal human eyes. *J Glaucoma* 2016;25(5):447-451.

22 Nadler Z, Wang B, Schuman JS, Ferguson RD, Patel A, Hammer DX, Bilonick RA, Ishikawa H, Kagemann L, Sigal IA, Wollstein G. In vivo three-dimensional characterization of the healthy human lamina cribrosa with adaptive optics spectral-domain optical coherence tomography. *Invest Ophthalmol Vis Sci* 2014;55(10):6459-6466.

23 Quigley HA, Addicks EM. Regional differences in the structure of the lamina cribrosa and their relation to glaucomatous optic nerve damage. *Arch Ophthalmol* 1981;99(1):137-143.

24 Huang D, Swanson EA, Lin CP, Schuman JS, Stinson WG, Chang W, Hee MR, Flotte T, Gregory K, Puliafito CA. Optical coherence tomography. *Science* 1991;254(5035):1178-1181.

25 Blumenthal EZ, Williams JM, Weinreb RN, Girkin CA, Berry CC, Zangwill LM. Reproducibility of nerve fiber layer thickness measurements by use of optical coherence tomography. *Ophthalmology* 2000;107(12):2278-2282.

26 Wollstein G, Schuman JS, Price LL, Aydin A, Stark PC, Hertzmark E, Lai E, Ishikawa H, Mattox C, Fujimoto JG, Paunescu LA. Optical coherence tomography longitudinal evaluation of retinal nerve fiber layer thickness in glaucoma. *Arch Ophthalmol* 2005;123(4):464-470.

27 Fortune B, Reynaud J, Wang L, Burgoyne CF. Does optic nerve head surface topography change prior to loss of retinal nerve fiber layer thickness: a test of the site of injury hypothesis in experimental glaucoma. *PLoS One* 2013;8(10):e77831.

28 Pollet-Villard F, Chiquet C, Romanet JP, Noel C, Aptel F. Structure-function relationships with spectral-domain optical coherence tomography retinal nerve fiber layer and optic nerve head measurements. *Invest Ophthalmol Vis Sci* 2014;55(5):2953-2962.

29 Deng S, Wang M, Yan Z, Tian Z, Chen H, Yang X, Zhuo Y. Autophagy in retinal ganglion cells in a rhesus monkey chronic hypertensive glaucoma model. *PLoS One* 2013;8(10):e77100.